

MRI Findings at the Bone-Component Interface in Symptomatic Unicompartmental Knee Arthroplasty and the Relationship to Radiographic Findings

Laura Jill Kleebblad, MD  · Hendrik A. Zuiderbaan, MD, PhD · Alissa J. Burge, MD · Mark J. Amirtharaj, BS · Hollis G. Potter, MD · Andrew D. Pearle, MD

Received: 9 May 2018/Accepted: 26 July 2018/Published online: 23 August 2018
© Hospital for Special Surgery 2018

Abstract *Background:* The most common modes of failure of cemented unicompartmental knee arthroplasty (UKA) designs are aseptic loosening and unexplained pain at short- to mid-term follow-up, which is likely linked to early fixation failure. Determining these modes of failure remains challenging; conventional radiographs are limited for use in assessing radiolucent lines, with only fair sensitivity and specificity for aseptic loosening. *Questions/Purposes:* We sought to characterize the bone-component interface of patients with symptomatic cemented medial unicompartmental knee arthroplasty (UKA) using magnetic resonance imaging (MRI) and to determine the relationship between MRI and conventional radiographic findings. *Methods:* This retrospective observational study included 55 consecutive patients with symptomatic cemented UKA. All underwent

MRI with addition of multiacquisition variable-resonance image combination (MAVRIC) at an average of 17.8 ± 13.9 months after surgery. MRI studies were reviewed by two independent musculoskeletal radiologists. MRI findings at the bone-cement interface were quantified, including bone marrow edema, fibrous membrane, osteolysis, and loosening. Radiographs were reviewed for existence of radiolucent lines. Inter-rater agreement was determined using Cohen's κ statistic. *Results:* The vast majority of symptomatic UKA patients demonstrated bone marrow edema pattern (71% and 75%, respectively) and fibrous membrane (69% and 89%, respectively) at the femoral and tibial interface. Excellent and substantial inter-rater agreement was found for the femoral and tibial interface, respectively. Furthermore, MRI findings and radiolucent lines observed on conventional radiographs were poorly correlated. *Conclusion:* MRI with the addition of MAVRIC sequences could be a complementary tool for assessing symptomatic UKA and for quantifying appearances at the bone-component interface. This technique showed good reproducibility of analysis of the bone-component interface after cemented UKA. Future studies are necessary to define the bone-component interface of symptomatic and asymptomatic UKA patients.

Level of Evidence: IV

Electronic supplementary material The online version of this article (<https://doi.org/10.1007/s11420-018-9629-1>) contains supplementary material, which is available to authorized users.

L. J. Kleebblad, MD (✉) · M. J. Amirtharaj, BS · A. D. Pearle, MD
Department of Orthopaedic Surgery, Sports Medicine and Shoulder Service, Hospital for Special Surgery, Weill Medical College of Cornell University,
535 East 70th Street,
New York, NY 10021, USA
e-mail: laurajillkleebblad@gmail.com

H. A. Zuiderbaan, MD, PhD
Department of Orthopaedic Surgery, Academic Medical Center
Utrecht,
Heidelberglaan 100,
3584 CX, Utrecht, Netherlands

A. J. Burge, MD · H. G. Potter, MD
Department of Radiology and Imaging, Hospital for Special Surgery,
535 East 70th Street,
New York, NY 10021, USA

Keywords MRI · unicompartmental knee arthroplasty · multiacquisition variable-resonance image combination (MAVRIC) · bone-component interface · implant integration

Introduction

The longevity of unicompartmental knee arthroplasty (UKA) is determined by the stability of the component fixation, lower-leg alignment, soft-tissue balance, and component position [5, 15]. Stable implant fixation with adequate cement penetration to underlying bone is essential in

preventing failure in cemented UKA [11, 27], most commonly through aseptic loosening and unexplained pain at short- to mid-term follow-up (likely linked to early fixation failure) [4–7]. Detecting the mode of failure in UKA remains challenging; the capacity of conventional radiographs in assessing radiolucent lines (RLL) is limited, with only fair sensitivity and specificity in detecting aseptic loosening [20].

Over the past decade, several studies have shown the diagnostic value of supplemental magnetic resonance imaging (MRI) in the evaluation of symptoms that arise after joint replacement [29, 32]. More specifically, MRI has been found useful in evaluating painful total knee arthroplasty (TKA), allowing assessment of the periprosthetic bone and soft tissues, which could influence clinical management [8, 26, 29, 31]. Conventional fast-spin-echo (FSE) techniques have improved visualization of periprosthetic soft tissues, although susceptibility artifacts can impair through-plane encoding of the signal and limit assessment of bone and soft tissues [29, 31]. Most recently, multiacquisition variable-resonance image combination (MAVRIC) MRI sequence has been shown to substantially reduce susceptibility artifacts near metallic implants. By mitigating through-plane misregistration, it allows identification of early and subtle changes, such as osteolysis and bone marrow edema, near the bone-prosthesis interface. Hayter et al. reported that MAVRIC visualization of the synovium is significantly improved over FSE imaging, with high sensitivity and specificity [13, 24]. Further, MAVRIC allows differentiation of certain synovial appearances associated with loosening and polyethylene wear and therefore can be valuable in the assessment of symptomatic patients [24]. Although multiple studies have assessed the bone-implant interface and soft-tissue changes around TKA, only a few small studies have evaluated the reliability or agreement of different MRI techniques around UKA [2, 25]. UKA is of interest because only a single knee compartment is replaced by a smaller prosthesis, compared with the multiple stabilizing pegs of TKA that can complicate the assessment of the bone-implant interface.

The aims of this retrospective observational study were to (1) describe and characterize the bone-implant interface in patients presenting with symptomatic medial UKA and (2) determine the inter-rater agreement of individual MRI findings at the bone-component interface. Also, the relationship between osseous findings on MRI and on radiographic

images was assessed. We hypothesized that MRI with MAVRIC would facilitate excellent visualization of the bone-implant interface due to its tomographic nature and superior contrast resolution with high inter-rater agreement for assessment of symptomatic UKA. We also expected that MRI findings would correlate poorly with conventional radiographic findings due to the expected diminished sensitivity of radiography.

Materials and Methods

After receiving institutional review board approval, an electronic registry search was performed using a prospective database, which included 874 medial UKAs. All surgeries were performed between September 2008 and March 2016 by the senior author (ADP). Patients who had been referred for MRI to evaluate symptomatic medial UKA at a minimum of 3 months after surgery were included in this study. From 87 cases identified, 19 were excluded due to an all-polyethylene inlay design of the tibial baseplate, 11 for lack of MAVRIC sequences for assessment, one for active infection, and one for history of amyloidosis. Data collected for the remaining 55 patients who had received a robotic-arm-assisted cemented metal-backed UKA (Stryker, Mahwah, NJ, USA) included age, sex, BMI, length of time since UKA surgery, indication for MRI, and re-operations.

All subjects underwent MRI using standard clinical protocols designed to minimize metallic susceptibility artifact between March 2012 and July 2016. MRI was performed on a General Electric 1.5T clinical scanner (Waukesha, WI, USA), using a dedicated extremity coil and the institution's routine clinical knee arthroplasty imaging protocol (Table 1), which is optimized for imaging tissues surrounding metallic hardware. This MRI protocol includes sagittal MAVRIC inversion-recovery and sagittal MAVRIC proton-density-weighted images, in addition to high-resolution axial, sagittal, and coronal proton-density-weighted FSE images obtained with metal artifact reduction parameter modifications. MAVRIC suppresses metal susceptibility artifact by combining individual three-dimensional image datasets at multiple frequency bands offset from the dominant resonant frequency utilizing a sum-of-squares algorithm to generate a final composite image, thereby mitigating through-plane distortions. This imaging

Table 1 Routine clinical imaging protocol for knee arthroplasty at 1.5 T

Parameter	Sagittal MAVRIC IR	Axial FSE	Sagittal FSE	Coronal FSE	Sagittal MAVRIC FSE
TR (ms)	4000–5000	4000–5000	4000–5000	4000–5000	4000–5000
TE (ms)	6	30	30	30	6
TI (ms)	150	NA	NA	NA	NA
BW (Hz/px)	488	488	488	488	488
NEX	0.5	4	4	4	0.5
FOV (cm)	20	16–18	16–18	16–20	20
Matrix	256 × 192	512 × 320	512 × 320	512 × 320	512 × 256
Slice/gap (mm)	3.6/0	3/0	2.5/0	4/0	3.6/0

BW bandwidth, *FOV* field-of-view, *FSE* fast spin echo, *Hz/px* Hertz per pixel, *IR* inversion recovery, *MAVRIC* multiacquisition variable-resonance image combination, *mm* millimeter, *ms* millisecond, *NEX* number of excitations, *TE* echo time, *TI* inversion time, *TR* repetition time, *NA* not applicable

Table 2 Indications for obtaining post-operative MRIs

Indication	Number of cases (<i>n</i> = 55)	Percentage
Unexplained pain	37	67.3%
Meniscal tear	4	7.3%
Chondral surfaces	3	5.5%
Loosening	2	3.6%
Integrity biceps femoris insertion	2	3.6%
Stress reaction	2	3.6%
Tibial spine fracture	1	1.8%
Integrity extensor mechanism	1	1.8%
Insert displacement	1	1.8%
Loose body	1	1.8%

algorithm provides good spatial resolution through FSE images, as well as superior suppression of susceptibility artifact though MAVRIC pulse sequences [13, 22].

MRI studies were retrospectively reviewed by two fellowship-trained musculoskeletal radiologists (AJB and HCP), with more than 5 and 15 years of experience, respectively, in MRI evaluation of joint arthroplasty.

Imaging studies were reviewed independently by both observers in a blinded fashion, with respect to multiple imaging features pertaining to the implant-bone interface, including the presence and severity of bone marrow edema, fibrous membrane formation and osteolysis. Bone marrow edema pattern manifests as relative signal hyperintensity within the medullary bone adjacent to the implant on fat-suppressed fluid-sensitive (MAVRIC inversion recovery) images. Fibrous membrane formation was defined as a thin isointense-to-hyperintense linear interface with a sclerotic osseous margin along the implant-bone interface. Osteolysis was defined as bulky, lobular, isointense-to-hyperintense foci with well-circumscribed sclerotic margins along the

Table 3 Categorization of the MRI findings using MAVRIC and FSE sequences

Findings	Tibial* (<i>n</i> = 55)	Femoral* (<i>n</i> = 55)
Bone marrow edema		
No	14 (25%)	16 (29%)
Mild (< 1 cm ²)	34 (62%)	26 (47%)
Moderate (1–2 cm ²)	5 (9%)	10 (18%)
Severe (> 1 cm ²)	2 (4%)	3 (5%)
Fibrous membrane		
No	6 (11%)	17 (31%)
Mild (< 33%)	31 (56%)	34 (62%)
Moderate (33–67%)	16 (29%)	3 (5%)
Severe (> 67%)	2 (4%)	1 (2%)
Osteolysis		
No	50 (91%)	47 (82%)
Focal	4 (7%)	8 (16%)
Diffuse	1 (2%)	1 (2%)
Loosening		
No	55 (100%)	54 (98%)
Loose	0 (0%)	1 (2%)

*The values are given as the number of components with the percentages in parentheses

implant interfaces. Bone marrow edema pattern was graded on a scale of 0 to 3, depending on the volume of marrow involved: 0 = no involvement, 1 = less than 1 cm³, 2 = 1 to 2 cm³, and 3 = more than 2 cm³. The extent of fibrous membrane formation was graded on a scale of 0 to 3, depending on the percentage of the implant interface involved, with 0 = no involvement, 1 = less than 33% involved, 2 = 33 to 67% involved, and 3 = more than 67% involved. Osteolysis was quantified as 0 = absent, 1 = focal, and 2 = diffuse. Loosening was defined as either circumferential bone resorption by fibrous membrane formation around the component or extensive osteolysis.

Radiographic evaluation was performed using our institutional Picture Archiving and Communication System (Sectra Imtec AB, Version 16, Linköping, Sweden). Anteroposterior (AP) and lateral radiographs, which corresponded to the MRI follow-up length, were compared to radiographs obtained 2 weeks post-operatively. All radiographs were acquired according to a standardized protocol, consisting of an AP weight-bearing view and lateral view, with knee in 30° of flexion [10, 18, 21]. A single assessor (LJK) assessed the presence of RLL and osteolysis on the AP and lateral radiographs, blinded to the MRI findings. Similar to previous studies, we determined the existence of tibial RLL using AP radiographs [10, 18, 21]. Femoral RLL was assessed using lateral radiographs, due to the limited visibility of the flat area along the anterior and posterior femoral condyle and the area surrounding the two pegs [17, 20]. Radiolucency was quantified as physiological or pathological RLL. Physiological RLL are well-defined, 1 to 2 mm thick, and accompanied with a radiodense line, in contrast to pathological RLL (more than 2 mm thick, poorly defined, and lacking a radiodense line) [9]. Osteolysis was defined as an irregularly shaped radiolucent zone along the bone-implant interface, irregularly demarcated from the surrounding bone. Osteolysis was quantified as focal or diffuse.

Analyses were performed using SPSS version 24 (SPSS Inc., Armonk, NY, USA). The following parameters were collected: gender, age, BMI, date of surgery, date of MRI and radiographic follow-up, and indication for MRI. They were assessed using descriptive statistics, consisting of mean, standard deviation (\pm), range, and frequency reported as percentage. Inter-rater agreement of MRI findings at the bone-component interface was determined using Cohen's kappa statistic (κ); the characterizing guidelines are 0.00–0.20, indicating poor agreement; 0.21–0.40, fair; 0.41–0.60, moderate; 0.61–0.80, substantial; and > 0.81, excellent [23]. Prior to this study, Li and colleagues showed high diagnostic accuracy of synovial appearances using MAVRIC, and therefore it was not reassessed [24]. Spearman correlation analyses were conducted to test for any relation between MRI and radiographic findings around each component. Statistical significance was set at $p < 0.05$.

Results

A total of 55 patients with symptomatic cemented metal-backed UKA were identified and included in this study. The mean age

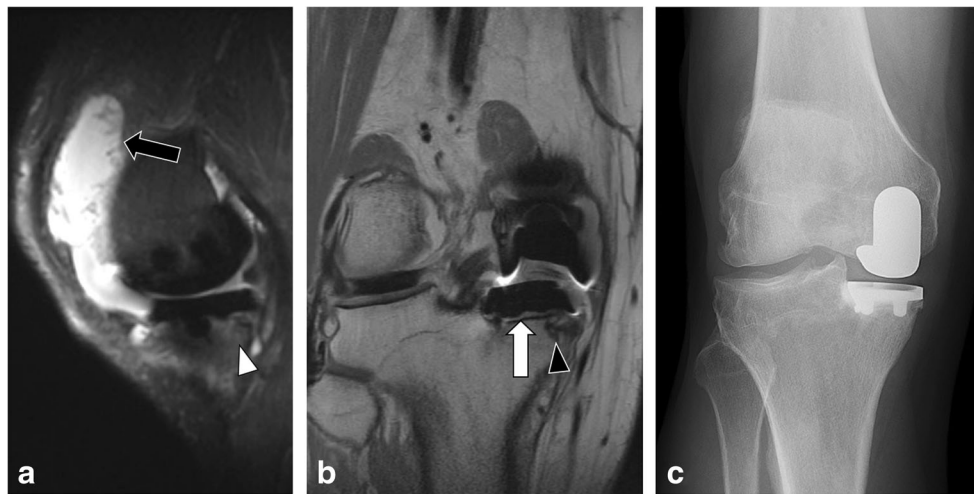


Fig. 1. Sagittal MAVRIC inversion-recovery (a) and coronal fast-spin-echo proton-density (b) images in a 55-year-old man with painful medial tibiofemoral unicompartmental knee arthroplasty show polymeric wear, with isointense debris containing synovitis (black arrow), tibial osteolysis (black arrowhead), and adjacent fibrous membrane formation (white arrow). Adjacent tibial marrow edema (white arrowhead) is compatible with superimposed stress reaction. Anteroposterior radiograph (c) was interpreted as negative.

was 59.7 ± 8.2 (range, 45.5–81.9) years, and BMI was $29.7 \pm 5.8 \text{ kg/m}^3$ (range, 18.3 to 46.0; one patient was morbidly obese). Of all patients, 26 (47%) were male and 29 (53%) female. All patients underwent a post-operative MRI including FSE and MAVRIC sequences at an average of 17.8 ± 13.9 -month post-surgery (when standard radiographs were unable to identify etiology). The most frequent indication for post-operative MRI was unexplained pain ($n = 37$, 67.3%). Other indications for MRI were findings of physical examination (Table 2).

MRI findings at both the tibial and femoral bone-implant interfaces are described in Table 3. In approximately half of patients (range, 47 to 62%) mild bone marrow edema pattern and fibrous membrane were observed (Fig. 1a, b; Fig. 3b, c). One patient's MRI showed diffuse osteolysis around the femoral component, which was also displaced (Fig. 2). No tibial components appeared loose on MRI.

The use of MRI with MAVRIC sequences showed excellent inter-rater agreement for assessment of the bone-component interface along the femoral component for all findings ($\kappa > 0.830$; 95% CI, 0.671–0.998) (Table 4). The inter-rater agreement of bone marrow edema and fibrous membrane at the tibial interface were substantial ($\kappa = 0.703$; 95% CI, 0.489–0.917 and $\kappa = 0.740$; 95% CI, 0.464–1.0, respectively). None of the tibial components appeared loose; therefore, no inter-rater agreement could be determined (Table 4).

The average time to conventional radiography after surgery was 17.6 ± 15.6 months, resulting in a mean time difference between MRI and radiograph of 2.3 ± 4.3 months. In total, 14 (25.5%) knees showed RLL, all categorized as physiological, except for one case (2%) that showed a displaced femoral component (Fig. 2). Of all knees with

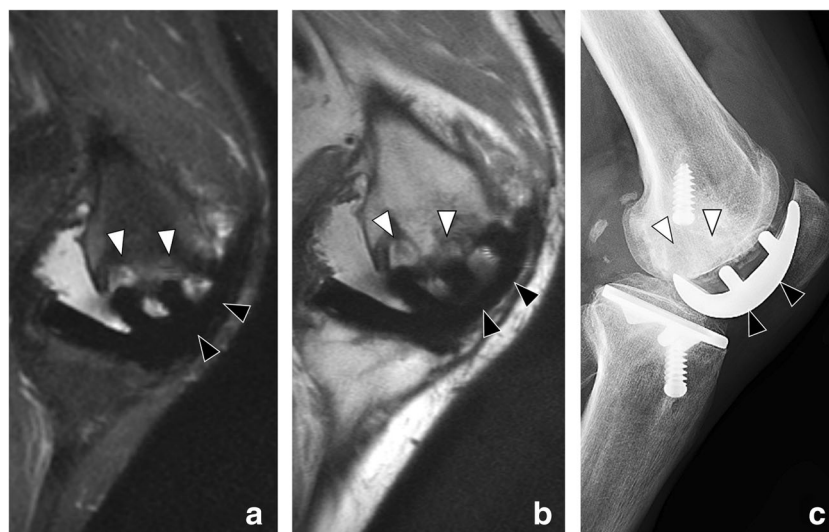


Fig. 2. Sagittal MAVRIC inversion-recovery (a) and sagittal MAVRIC proton-density-weighted (b) images in a 54-year-old man with painful medial tibiofemoral unicompartmental knee arthroplasty demonstrate circumferential osseous resorption (white arrowheads) along the femoral component (black arrowheads), resulting in component loosening with anterior displacement. Lateral radiograph (c) demonstrates component displacement (black arrowheads), although the extent of osseous resorption (white arrowheads) is more clearly appreciated on MRI.

Table 4 Inter-rater agreement of the presence of MRI findings at the bone-component interface

	Inter-rater agreement (%)	Cohen's κ	95% confidence interval
Femoral component			
Bone marrow edema	96.4	0.912	0.792–1.0
Fibrous membrane	92.7	0.830	0.671–0.998
Osteolysis	98.1	0.936	0.813–1.0
Loosening	100	1.0	–
Tibial component			
Bone marrow edema	89.1	0.703	0.489–0.917
Fibrous membrane	94.5	0.740	0.464–1.0
Osteolysis	100	1.0	–
Loosening	–	–	–

physiological RLL, seven (14.5%) showed RLL below the tibial baseplate, six (10.9%) showed only femoral RLL, and one (1.8%) had both tibial and femoral RLL. Forty-one (74.5%) patients did not show any RLL around either component. Radiographic osteolysis was not observed.

Spearman correlation analyses assessing the relation between the MRI appearances and radiographic findings showed a weak correlation between tibial RLL on radiographs and osteolysis and loosening on MRI (correlation coefficient: 0.262, $p = 0.040$ and 0.329, $p = 0.015$, respectively). No additional correlations were found (Table 5).

In one patient, the MRI and radiographic assessment revealed a displaced femoral component requiring revision of the femoral component and insert (Fig. 2). Moreover, 12 re-operations were performed, of which nearly all were arthroscopic procedures (Table 6).

Discussion

MRI with MAVRIC technique showed good reproducibility in analyzing the implant-bone interface after cemented medial UKA. The inter-rater agreement of assessing bone marrow edema, fibrous membrane, osteolysis, and loosening was excellent around the femoral component and substantial at the tibial interface. Furthermore, a poor correlation was found between MRI findings and RLL using conventional radiographs. These data support the application of these

imaging techniques to the assessment of implant integration (Figs. 1 and 3).

The current study has several limitations. First, by including consecutive patients undergoing MRI for symptomatic UKA, selection bias was considered low. However, no asymptomatic patients were included, which might still lead to a sampling bias. Furthermore, the MRIs after UKA were obtained for different indications. Although most patients had painful UKA (67%), these findings do not relate directly to a specific subgroup. Despite this limitation, it provided the ability to detect and report the prevalence of specific features of symptomatic UKA. Another limitation was that the preserved knee compartments and other anatomical structures were not assessed in this study. However, Heyse et al. have showed excellent inter-rater agreement for the cruciate and collateral ligaments, lateral meniscus, and cartilage surfaces of the non-surgical areas following UKA [16]. Finally, this study is limited by lack of functional outcomes, but any subsequent clinical treatment following MRI was reported.

In accordance with our main findings, Malcherczyk and colleagues found excellent inter-rater reliability for the femoral bone-component interface and satisfactory results at the tibial interface of metal-backed UKA implants [25]. Evaluation of all components was performed by applying a new scoring system in which the visibility and gap between component and underlying bone was assessed using FSE sequences. The authors showed 40% of the zones around the tibial component could not be evaluated due to metal

Table 5 Relationship between conventional radiography and MRI findings at the bone-component interface divided by component

Radiograph	MR finding	Correlation coefficient*	p value
Femoral component			
Radiolucency ($n = 6$)	Bone marrow edema	0.113	0.417
	Fibrous membrane	0.125	0.368
	Osteolysis	–0.147	0.287
	Loosening	–	–
Tibial component			
Radiolucency ($n = 8$)	Bone marrow edema	0.156	0.259
	Fibrous membrane	0.027	0.845
	Osteolysis	0.280	0.040
	Loosening	0.329	0.015

*Spearman correlation, two-tailed

Table 6 Specification of the 12 reoperations performed subsequent to MRI

Patient	Reoperation
F, 51 years	PLM, synovectomy, debridement fat pad*
M, 53 years	PLM, chondroplasty of trochlea, removal loose body*
M, 55 years	PLM, synovectomy, chondroplasty of PF joint*
M, 57 years	Debridement, chondroplasty of trochlea and patella*
F, 58 years	PLM, chondroplasty of PF joint*
M, 58 years	PLM, chondroplasty of trochlea, debridement, femoral subchondroplasty*
F, 61 years	PLM, removal loose body*
F, 62 years	Debridement, PLM, chondroplasty of PF joint*
M, 62 years	Debridement, removal loose body*
M, 66 years	Arthrotomy, internal fixation of insufficiency stress fracture
M, 70 years	Removal loose body, chondroplasty*
F, 73 years	Removal of loose body*

*Arthroscopic procedures

F female, M male, PF patellofemoral, PLM partial lateral meniscectomy

artifact, resulting in a κ value of 0.722 on the tibial side [25]. Although interfaces are not necessarily artifact-free, MAVRIC results in a significant decrease in susceptibility artifact, usually resulting in improved visualization of implant interfaces relative to conventional sequences. Hayter and colleagues compared periprosthetic bone visualization between MAVRIC and FSE images in 21 TKA patients, and found significantly better visualization of bone on MAVRIC images than on FSE images ($p < 0.01$) [13]. Therefore, they concluded that MAVRIC complements the information obtained from FSE images and may be useful in assessing osteolysis at the bone-component interface.

The κ values for bone marrow edema and fibrous membrane along the tibial interface were 0.703 and 0.740, respectively. Both are considered important in

symptomatic UKA, as they could be indicative of aseptic loosening. Several authors have suggested that aseptic loosening is caused by micromotion between the implant or cement surface and the bone, leading to fibrous membrane formation, trabecular microtrauma, and subsequent bone marrow edema [3, 8]. Therefore, the proposed cause of post-operative bone marrow edema is increased bone strain, which has been associated with component alignment and fixation technique [8, 12, 19, 30]. Aseptic loosening can result from poor initial fixation, post-operative mechanical disruption of fixation, or biologic failure of fixation secondary to polyethylene wear and osteolysis [1, 32]. Although findings of loosening have been described for multiple imaging modalities, prosthetic loosening has mostly remained a clinical diagnosis. In large part, imaging findings of all modalities are considered secondary, but studies have shown MRI findings supportive of a diagnosis of loosening when suspected [28, 31, 33]. Therefore, the term *loosening* is recommended for cases where MRI demonstrates circumferential osseous resorption and signs of implant displacement, subsidence, or rotation [8].

Conventional radiographs can help detect gross prosthetic malposition, radiolucencies, and fractures [26], but they hold little value in the detection of the more common but subtle osseous abnormalities such as early loosening, minor implant malposition, infection, stress fractures, or early-stage osteoarthritis. Therefore, several authors have emphasized the additive value of MRI to radiographic imaging in determining the etiology of painful total joint arthroplasty [14, 15, 24, 26, 31]. Sofka et al. found that prospective and retrospective radiographs were non-contributory in the evaluation of painful TKA but observed varied and often multiple MRI findings in these knees, leading to subsequent clinical treatment in 20 patients [31]. A few studies have noted the very limited value of conventional radiographs in

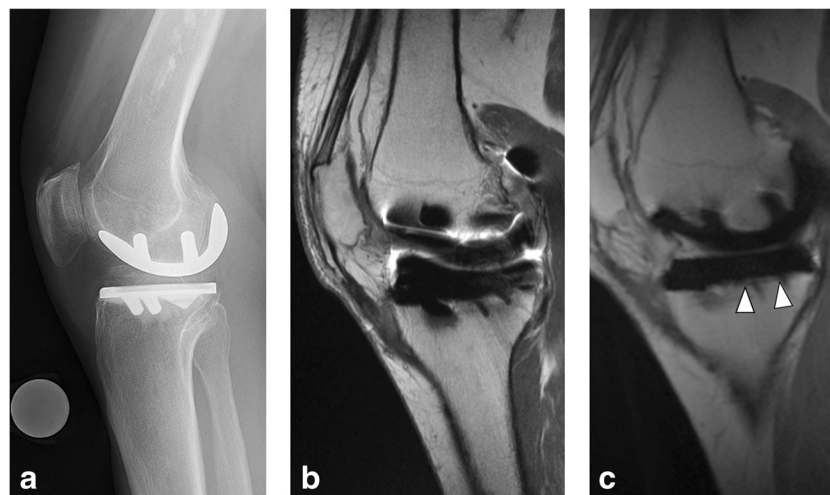


Fig. 3. Lateral radiograph (a) and sagittal proton-density (b) images in a 57-year-old woman with painful medial tibiofemoral unicompartmental knee arthroplasty show no evidence of periprosthetic bone resorption; however, sagittal MAVRIC proton-density (c) image demonstrates a focal area of fibrous membrane formation along the tibial tray (white arrowheads).

diagnosing painful UKA [2, 28]. In this study, only a poor correlation was found between radiographic and MRI features, which could indicate that symptomatic UKA may be inadequately assessed on radiographs alone. These findings were consistent with those of Park et al., which showed MRI examination was instrumental in a diagnosis that went undetected on radiographs for all 28 symptomatic UKA patients [28]. They concluded that MRI is an effective imaging technique that provides greater insight into the etiology of the symptomatic patient following UKA.

MRI with the addition of MAVRIC could be a valuable complement to radiographic evaluation in assessing symptomatic medial UKA and quantifying appearances at the bone-implant interface. However, future studies are necessary to define the bone-component interface of symptomatic and asymptomatic UKA patients. Additionally, excellent inter-rater agreement was found for the femoral bone-component interface and substantial agreement for the tibial bone-component interface. This MRI protocol may be helpful in detecting changes around symptomatic cemented UKA, especially in cases of unremarkable radiographic findings.

Compliance with Ethical Standards

Conflict of Interest: Laura J. Kleebblad, MD, Hendrik A. Zuiderbaan, MD, PhD, Alissa J. Burge, MD, Mark J. Amirtharaj, BS, declare that they have no conflicts of interest. Hollis G. Potter, MD, reports receiving grants from GE Healthcare, during the conduct of the study. Andrew D. Pearle, MD, reports receiving personal fees from Stryker Corporation and Exactech and personal fees from Zimmer Biomet, outside the submitted work.

Human/Animal Rights: All procedures followed were in accordance with the ethical standards of the responsible committee on human experimentation (institutional and national) and with the Helsinki Declaration of 1975, as revised in 2013.

Informed Consent: Informed consent was waived from all patients for being included in this study.

Required Author Forms Disclosure forms provided by the authors are available with the online version of this article.

References

1. Abu-Amer Y, Darwech I, Clohisy JC. Aseptic loosening of total joint replacements: mechanisms underlying osteolysis and potential therapies. *Arthritis Res Ther*. 2007;9(Suppl 1):S6.
2. Agten CA, Del Grande F, Fucentese SF, Blatter S, Pfirrmann CWA, Sutter R. Unicompartamental knee arthroplasty MRI: impact of slice-encoding for metal artefact correction MRI on image quality, findings and therapy decision. *Eur Radiol*. 2015;25(7):2184–2193.
3. Berkowitz JL, Potter HG. Advanced MRI techniques for the hip joint: focus on the postoperative hip. *Am J Roentgenol*. 2017;209(3):534–543.
4. Chou DTS, Swamy GN, Lewis JR, Badhe NP. Revision of failed unicompartamental knee replacement to total knee replacement. *Knee*. 2012;19(4):356–359.
5. Citak M, Dersch K, Kamath AF, Haasper C, Gehrke T, Kendoff D. Common causes of failed unicompartamental knee arthroplasty: a single-centre analysis of four hundred and seventy one cases. *Int Orthop*. 2014;38(5):961–965.
6. van der List JP, Zuiderbaan HA, Pearle AD. Why do medial unicompartamental knee arthroplasties fail today? *J Arthroplasty*. 2016;31(5):1016–1021.
7. Epinette J-A, Brunschweiler B, Mertl P, Mole D, Cazenave A, French Society for Hip and Knee. Unicompartamental knee arthroplasty modes of failure: wear is not the main reason for failure: a multicentre study of 418 failed knees. *Orthop Traumatol Surg Res*. 2012;98(6 Suppl):S124–30.
8. Fritz J, Lurie B, Potter HG. MR Imaging of knee arthroplasty implants. *Radiographics*. 2015;35(5):1483–1501.
9. Goodfellow JW, Kershaw CJ, Benson MK, O'Connor JJ. The Oxford Knee for unicompartamental osteoarthritis. The first 103 cases. *J Bone Joint Surg Br*. 1988;70(5):692–701.
10. Gulati A, Chau R, Pandit HG, et al. The incidence of physiological radiolucency following Oxford unicompartamental knee replacement and its relationship to outcome. *J Bone Joint Surg Br*. 2009;91(7):896–902.
11. Halawa M, Lee AJ, Ling RS, Vangala SS. The shear strength of trabecular bone from the femur, and some factors affecting the shear strength of the cement-bone interface. *Arch Orthop Trauma Surg*. 1978;92(1):19–30.
12. Hayashi D, Englund M, Roemer FW, et al. Knee malalignment is associated with an increased risk for incident and enlarging bone marrow lesions in the more loaded compartments: The MOST study. *Osteoarthritis Cartil*. 2012;20(11):1227–1233.
13. Hayter CL, Koff MF, Shah P, Koch KM, Miller TT, Potter HG. MRI after arthroplasty: Comparison of MAVRIC and conventional fast spin-echo techniques. *Am J Roentgenol*. 2011;197(3):405–411.
14. Hayter CL, Gold SL, Koff MF, et al. MRI findings in painful metal-on-metal hip arthroplasty. *Am J Roentgenol*. 2012;199(4):884–893.
15. Heyse TJ, Chong LR, Davis J, Boettner F, Haas SB, Potter HG. MRI analysis of the component-bone interface after TKA. *Knee*. 2012;19(4):290–294.
16. Heyse TJ, Figiel J, Hähnlein U, et al. MRI after unicondylar knee arthroplasty: the preserved compartments. *Knee*. 2012;19(6):923–926.
17. Hooper GJ, Maxwell AR, Wilkinson B, et al. The early radiological results of the uncemented Oxford medial compartment knee replacement. *J Bone Joint Surg Br*. 2012;94(3):334–338.
18. Hooper N, Snell D, Hooper G, Maxwell R, Frampton C. The five-year radiological results of the uncemented Oxford medial compartment knee arthroplasty. *Bone Joint J*. 2015;97-B(10):1358–1363.
19. Jacobs CA, Christensen CP, Karthikeyan T. Subchondral bone marrow edema had greater effect on postoperative pain after medial unicompartamental knee arthroplasty than total knee arthroplasty. *J Arthroplasty*. 2016;31(2):491–494.
20. Kalra S, Smith TO, Berko B, Walton NP. Assessment of radiolucent lines around the Oxford unicompartamental knee replacement: sensitivity and specificity for loosening. *J Bone Joint Surg Br*. 2011;93(6):777–781.
21. Kleebblad LJ, van der List JP, Zuiderbaan HA, Pearle AD. Regional femoral and tibial radiolucency in cemented unicompartamental knee arthroplasty and the relationship to functional outcomes. *J Arthroplasty*. 2017;32(11):3345–3351.
22. Koff MF, Shah P, Potter HG. Clinical implementation of MRI of joint arthroplasty. *Am J Roentgenol*. 2014;203(1):154–161.
23. Landis JR, Koch GG. The measurement of observer agreement for categorical data. *Biometrics*. 1977;33(1):159.
24. Li AE, Sneag DB, Iv HGG, Johnson CC, Miller TT, Potter HG. Total Knee Arthroplasty: diagnostic accuracy of patterns of synovitis at MR imaging 1. *Radiology*. 2016;281(2):1–8.

25. Malcherczyk D, Figiel J, Hahnlein U, Fuchs-Winkelmann S, Efe T, Heyse TJ. MRI following UKA: The component-bone interface. *Acta Orthop Belg.* 2015;81(1):84–89.
26. Mandalia V, Eyres K, Schranz P, Toms AD. Evaluation of patients with a painful total knee replacement. *J Bone Jt Surg Br.* 2008;90-B(3):265–271.
27. Mukherjee K, Pandit H, Dodd CAF, Ostlere S, Murray DW. The Oxford unicompartmental knee arthroplasty: a radiological perspective. *Clin Radiol.* 2008;63(10):1169–1176.
28. Park CN, Zuiderbaan HA, Chang A, Khamaisy S, Pearle AD, Ranawat AS. Role of magnetic resonance imaging in the diagnosis of the painful unicompartmental knee arthroplasty. *Knee.* 2015;22(4):341–346.
29. Potter HG, Foo LF. Magnetic resonance imaging of joint arthroplasty. *Orthop Clin North Am.* 2006;37(3):361–373.
30. Small SR, Berend ME, Rogge RD, Archer DB, Kingman AL, Ritter MA. Tibial loading after UKA: Evaluation of tibial slope, resection depth, medial shift and component rotation. *J Arthroplasty.* 2013;28(9 SUPPL):179–183.
31. Sofka CM, Potter HG, Figgie M, Laskin R. Magnetic resonance imaging of total knee arthroplasty. *Clin Orthop Relat Res.* 2003;(406):129–135.
32. Talbot BS, Weinberg EP. MR imaging with metal-suppression sequences for evaluation of total joint arthroplasty. *Radiographics.* 2015;36(1):209–225.
33. Temmerman OPP, Rajmakers PGHM, Berkhof J, Hoekstra OS, Teule GJJ, Heyligers IC. Accuracy of diagnostic imaging techniques in the diagnosis of aseptic loosening of the femoral component of a hip prosthesis: a meta-analysis. *J Bone Joint Surg Br.* 2005;87(6):781–785.